

Design and Fabrication of Printed Electrowetting-on-Dielectric Device

Bongmin Kim¹, Seung Jun Lee^{1,2}, Inyoung Kim¹, and Taik-Min Lee^{1,#}

¹ Department of Printed Electronics, Advanced Manufacturing Systems Research Division, Korea Institute of Machinery & Materials, 156, Gajeongbuk-ro, Yuseong-gu, Daejeon, 305-343, South Korea

² Device and System Center, Samsung Advanced Institute of Technology (SAIT), 130, Samsung-ro, Yeongtong-gu, Suwon-si, Gyeonggi-do, 443-803, South Korea

Corresponding Author / E-mail: taikmin@kimm.re.kr, TEL: +82-42-868-7451, FAX: +82-42-868-7176

KEYWORDS: EWOD, Electrowetting, Electrowetting-on-dielectric, Printed EWOD, Printed electronics

Due to the expensive price of the fabrication process of the existing semiconductor technology, printing technology has become the center of much attention in research as a micro fabrication technology. Among printing technologies, the rReverse-offset-printing (ROP) method that can achieve high resolution and complicated shape patterns is utilized to fabricate the electrowetting-on-dielectric (EWOD) device, which has been widely researched for the control small-scale droplets. The EWOD device consists of three-layers which were successfully fabricated by the solution-based process. As a metal layer, Ag-ink was printed on the glass substrate by the ROP method. On top of this layer, a polymer solution (polyvinylphenol, PVP) was spin-coated as a dielectric layer, which has a high dielectric strength (100 V/mm) and high dielectric constant (3.9) compared to other spin-coatable dielectric materials. The Teflon solution was spin-coated on top of the dielectric layer to deposit a hydrophobic surface. Using the printed EWOD device, the transport of micro-size droplets was successfully demonstrated.

Manuscript received: June 8, 2014 / Revised: October 30, 2014 / Accepted: February 1, 2015

1. Introduction

Electrowetting-on-dielectric (EWOD) is a method used for modifying the wetting properties of a droplet on an insulator-coated electrode by applying a voltage to the droplet and thus changing its contact angle.^{1,2} The change of the contact angle can occur reversibly and quickly, depending on the applied voltage. It typically accompanies low energy consumption, since it is basically caused by an electrostatic phenomenon. For this reason, EWOD has been utilized in the wide range of applications, including liquid lenses,³ liquid prism,⁴ electronic display,⁵ and droplet-based microfluidics.⁶ So far, most EWOD-based devices have been fabricated using traditional semiconductor technology such as photolithography, wet/dry etching, and chemical/physical vapor deposition. However, the technology requires expensive equipment within clean room facilities and has difficulties on fabrication of flexible and large-scale devices.

Recently, printing technology has become the center of much attention in research as a micro fabrication technology owing to outstanding advantages such as lower production cost, flexibility, and printability on a large-area substrate, compared to the semiconductor technology.^{7,8} These benefits make the printed electronics technology

applicable to the development of elements such as organic photovoltaic (OPV) cells,^{9,10} radio frequency identification,¹¹ and super capacitors.¹² Among various printing methods, reverse offset printing (ROP) method features good precision, fine line width, and uniform thickness of the printed pattern, allowing for sophisticated form patterns.¹³ These advantages make it ideal for the fabrication of electrodes for EWOD devices.

To fabricate the EWOD device, a good quality of dielectric layer should be coated on the electrode for preventing electrolysis.¹⁴ Based on the semiconductor technology, various dielectric layers with good dielectric performance, such as silicon oxide (SiO₂), silicon nitride (Si₃N₄), and Parylene-C, have been deposited over the electrode through a chemical vapor deposition (CVD) process using expensive deposition equipment. In order for EWOD devices created via printed electronics technology to have greater competitiveness for industrial applications, however, a solution-based process is required for the deposition of a dielectric layer. For coating the dielectric layer on an electrode, the solution-based process utilizes the spin-coating method which benefits low cost and simple fabrication method. Materials available for a solution-based process for the EWOD dielectric layer include Teflon, PDMS, and polyimide. Teflon can serve not only as a

dielectric layer, but also as a hydrophobic layer, thus requiring no coating process later on. PDMS and polyimide provide the ability to implement a dielectric layer at a lower cost compared to the Teflon. However, the dielectric strength of these dielectric materials suitable for the solution-based process is lower than that of the dielectric materials processed by CVD process. Therefore, the spin-coatable dielectric material with high dielectric strength is required for low cost and easy fabrication.

In this study, we present the design and fabrication of the first EWOD device using printed electronics technique. The electrode array for EWOD device is fabricated based on the reverse offset printing (ROP) method. A dielectric layer and a hydrophobic layer are sequentially coated on the surface of the electrode based on the spin-coating method. All fabrication processes are based on the solution-based process. Using the printed EWOD device, we demonstrate the droplet transport.

2. Design and Materials of Printed EWOD Device

2.1 Principle of Electrowetting-on-dielectric (EWOD)

Electrowetting, or electrowetting-on-dielectric (EWOD)^{1,2} is a phenomenon in which the contact angle of a sessile droplet on an insulator-coated electrode surface is electrically changed. When voltage is applied to the droplet, the electrical force results in the reduction of its contact angle.¹ The degree of contact angle change depends on the level of voltage applied as illustrated in Lippmann-Young's equation (equation (1)).

$$\cos \theta_E = \cos \theta_Y + \frac{\epsilon_0 \epsilon_d V^2}{2d\gamma} = \cos \theta_Y + \frac{\epsilon_0 \epsilon_d E_d^2 d}{2\gamma} \quad (1)$$

where θ_Y is Young's contact angle of a droplet, θ_E is the contact angle when voltage is applied, ϵ_0 is vacuum permittivity, ϵ_d is dielectric constant, d is thickness of dielectric layer, γ is surface tension of a droplet, V is applied voltage, and E_d is electric field inside a dielectric layer (V/d). Eq. (1) indicates that when the dielectric constant is large and the thickness of dielectric layer is thin with an applied voltage fixed, the degree of the contact angle change increases. Also, Eq. (1) indicates that when the strength of the electric field inside the dielectric layer is greater than the dielectric strength, a breakdown can occur. It is therefore imperative to choose a material with high dielectric strength for use in the dielectric layer in order to increase the robustness of the device. In general, the greater the dielectric constant of the material used for the dielectric layer, the lower the level of dielectric strength. It is therefore imperative to choose a layer with a balanced dielectric constant and dielectric strength for the fabrication of EWOD devices.

2.2 Two configurations of EWOD devices

There are two kinds of configurations in EWOD to manipulate droplets using electrowetting: the single plate configuration¹⁵ and the two-parallel plate configuration^{6,16} (Fig. 1). The single plate configuration has only a base plate with an array of discrete electrodes (Fig. 1(a)). A dielectric layer is deposited over the electrode plate to prevent electrolysis of a droplet when the voltage is applied. Subsequently, a hydrophobic is coated to increase the contact angle of droplets and to

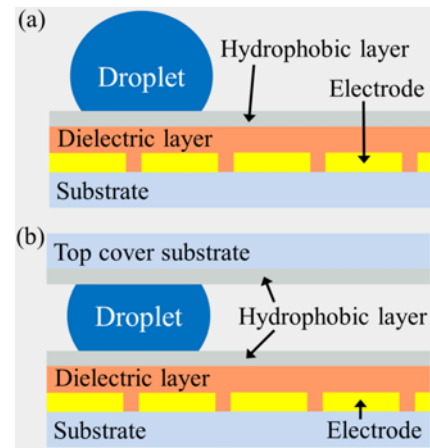


Fig. 1 Two configurations of EWOD devices: (a) Single-plate and (b) two-parallel plate configurations

reduce contact angle hysteresis. When a voltage is sequentially applied to the discrete electrode of the base plate beneath a sessile droplet, the droplet moves along the electrode activated. However, in the two-parallel plate configuration, a cover plate (including an electrode or not) coated with a hydrophobic layer is additionally utilized (Fig. 1(b)). Droplets are sandwiched between the base plate and cover plate. For droplet transport, a voltage is sequentially applied to the electrode of the base plate like the single-plate configuration. When the cover plate includes an electrode, a reference voltage is applied to the cover plate for the droplet transport. In this work, we designed two-parallel plate EWOD device consisting of a cover plate and a base plate as shown in Fig. 1(b).

2.3 Electrode design

Reverse offset printing (ROP) method (See Section 3.2.) is used to fabricate an electrode for EWOD device. The size and shape of the electrode are determined based on the features of the ROP method. The electrode consists of four parts: 1) an electrode array where droplets are manipulated, 2) a pad electrode through which voltage is applied to the electrode array, 3) a thin line electrode between the electrode array and the pad and 4) a gap between two discrete electrodes of the electrode array (Fig. 2). The electrode has both large-area pattern (electrode array and pad electrode) and line pattern (line electrode and gap). Here, the size of a discrete electrode of the array is related with the droplet volume handled in EWOD device. The width of the thin line electrode can affect the path of moving droplet. Thus the small line width results in better control over the path of moving droplet. The gap size between two discrete electrodes of the array is important parameter in designing the electrode. As the gap size becomes smaller, the droplet easily and successively moves from one to another electrode surface. Consequently, in printing electrode, the size of the line electrode and the gap is mainly affected by the feature of ROP method because a smaller printing size entails greater difficulty in printing. The minimum size of a pattern printable under the ROP method is about 5-10 μm . Considering the features of electrode and ROP method, we design the EWOD device. Table 1 shows the specification of size of the electrode for the printed EWOD device.

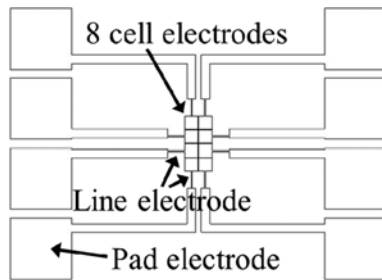


Fig. 2 Design of EWOD device consisting of three parts; 1) electrode array (8 cells) on which a droplet is moving, 2) node connecting a cell electrode with a pad electrode and 3) pad electrodes for applying voltage

Table 1 Size of electrode for the printed EWOD device

Part of electrode	Size (mm)
Length of a discrete electrode	1.41
Length of a pad electrode	6.91
Width of a line electrode	0.01 or 0.1
Electrode gap	0.17 or 0.05

2.4 Materials for printing and solution-based process

All processes for the fabrication of the EWOD device are solution-based process. The material used for the fabrication of the electrode is Ag nanoparticles ink (Ag-NPs ink, Ag content 39wt%, Advanced Nano Products Co., Ltd.) suitable for ROP method. The solution used to place a dielectric layer over the electrode plate is polyvinylphenol (PVP, Sigma-Aldrich). This solution is a widely used as a dielectric layer for organic transistors.^{17,18} The PVP solution is more affordable and has greater dielectric constant (3.9) and higher dielectric strength (>100 V/mm) than the dielectric materials (Teflon, PDMS, Polyimide) that are commonly used for solution-based process. The PVP solution is deployed through a solution-based process for the deposition of a dielectric layer in EWOD. Comparison with dielectric layer materials placed via the traditional CVD process also reveals similar advantages in the PVP material. For coating a hydrophobic layer, Teflon solution is utilized.

2.5 Specification of a printed EWOD device

The material, fabrication method and target thickness for each layer of the EWOD plate fabricated based on a printing process and a solution-based process are as shown in Table 2. The electrode layer listed in the first row of Table 2 is created via the ROP method, and the target thickness of the electrode is less than 1 μm . If the electrode is too thick, droplets have difficulty in crossing over the high electrode step height.¹⁹ By contrast, if the electrode is too thin, there is a possibility that, due to the limited capability of the printing process, its sheet resistance increases to a level where it does not fulfill its role. The dielectric layer and the hydrophobic layer are placed on the electrode surface via spin coating. The target thickness of the dielectric layer is a minimum 1 μm thicker than the electrode. If the electrode is thicker than the dielectric layer, a breakdown may easily occur at the edge of the electrode, affecting droplet transport.¹⁹ The target thickness of the hydrophobic layer is around 100 nm thinner than the dielectric layer.

Table 2 Materials, methods and target thickness of each layer of EWOD device

Layer	Material	Method	Target thickness (μm)
1 st electrode layer	Ag-ink	ROP	<1
2 nd dielectric layer	PVP	Spin-coating	>1
3 rd hydrophobic layer	Teflon	Spin-coating	<0.1

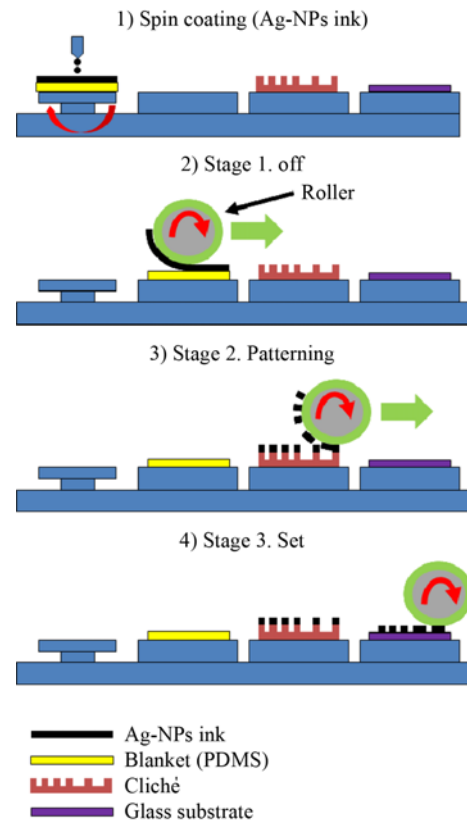


Fig. 3 Reverse offset printing (ROP) process

3. Fabrication Procedure

3.1 Preparation of electrode material

Pre-treatment of the electrode solution (Ag-NPs ink) was conducted before the ROP process to ensure that the thickness of the electrode is uniform. Subsequently, the electrode solution was coated via spin coating. First of all, the Ag-NPs ink was sonicated for 30 minutes. Then, the Ag-NPs ink was filtered through PTFE (0.2 mm) to remove large aggregated particles remaining within the sonicated Ag-NPs ink.

3.2 Reverse offset printing process for electrode fabrication

In order to make the thickness of the electrode less than 1 μm , the spin-coating method is utilized as the first step before the ROP process. Thus, the printing process of the electrode consists of the four steps (Spin-coating process + three stages (off-patterning-set) of ROP process as shown in Fig. 3): 1) The Ag-NPs ink solution was spin coated over the blanket substrate (PDMS) surface at 6000 rpm for 10 seconds. 2) At stage 1 of ROP machine, the entire electrode material spin-coated

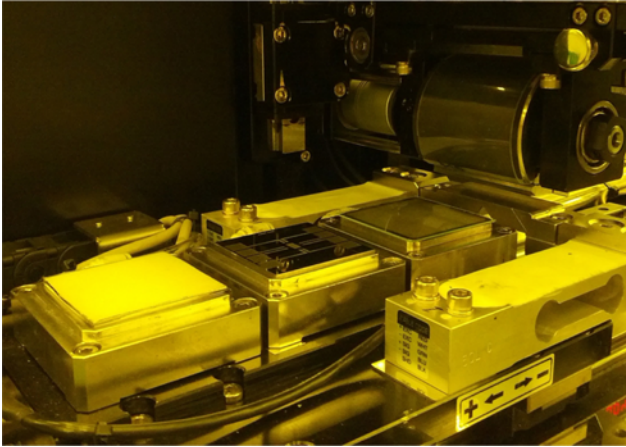


Fig. 4 Reverse offset printing (ROP) machine

Table 3 Reverse offset printing condition for Ag electrode

Parameter	Off	Patterning	Set
Speed (mm/s)	10	10	5
Pressure (kgf)	6	2	6

over the base blanket was transferred to the surface of the roller. 3) At stage 2, the material transferred to the roller surface came in contact with the cliché and was then transferred to the embossing of the plate. 4) At stage 3, any pattern remaining on the roller surface that has not been transferred to the cliché was transferred to the base glass substrate. The electrode was printed onto a glass plate using ROP equipment (Fig. 4). The electrode was then baked on a hot plate or in the oven at 300 degrees for 30 minutes to sinter the Ag-NPs ink.

The most important stage of all three stages during the ROP process is the second stage at which the pressure and rotation speed of the roller are the most critical parameters. Since the electrode consists of a large area pattern and a thin line pattern, the two conditions of pressure and speed must be experimentally balanced. If the roller pressure applied to the cliché is greater than the acceptance level, not only the embossing but also the intaglio of the cliché comes in contact with the roller ink, resulting in the transfer of all the ink on the roller surface to the cliché and no transfer of the ink to the glass surface at stage 3. If the roller moves too fast, sufficient cohesion force fails to fully form within the ink or adhesion force between the ink and the embossing of the cliché fails to fully develop, resulting in a failure of printing the border between the embossing and the intaglio to tear.²⁰ As a result, there is ambiguity between the face pattern and the line pattern. In the first and the third stages, pressure and speed over a certain level are the only two requirements for printing. Conditions in each stage of the ROP process are as shown in Table 3.

3.3 Dielectric and hydrophobic layer

The dielectric layer and the hydrophobic layer are prepared as follows. PVP powder ($M_w = 20$ k) is dissolved in the propylene glycol methyl ether acetate (PGMEA) solution. Then cross-linking agent poly (melamine-co-formaldehyde) of PVP was dissolved in the solution. This solution (20wt% PVP solution) was spin-coated at 1000 rpm for 30 seconds to deposit a dielectric layer over the surface of the printed

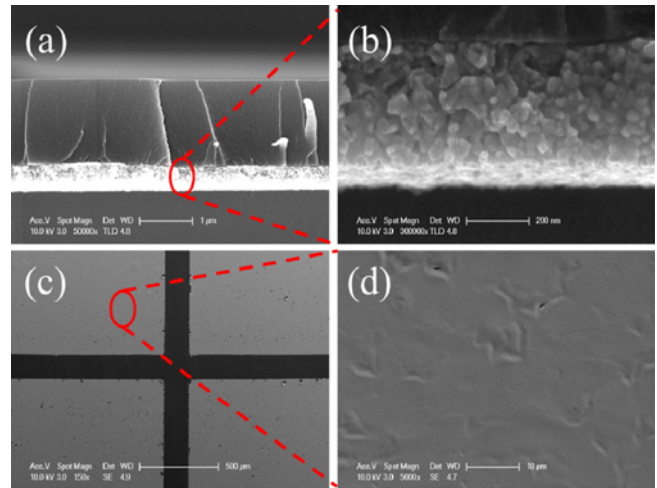


Fig. 5 SEM images of a printed EWOD device: (a) Side view of an Ag electrode coated with PVP dielectric layer (scale bar = 1 μ m), (b) Side view of an electrode consisting of Ag nanoparticles (scale bar = 200 nm), (c) Top view of an electrode with 170 μ m gap (scale bar = 500 μ m) and (d) Top view of an electrode surface (scale bar = 10 μ m)

electrode. The dielectric layer was cured on a hot plate at 180°C for 20 minutes. Subsequently, 1.9wt% Teflon solution was spin-coated at 2000 rpm for 30 seconds to allow the hydrophobic layer to be coated over the dielectric layer. The hydrophobic layer was then baked on a hot plate at 120°C for 1 minute.

3.4 Evaluation of fabrication

We examined the characteristics of the electrode, the dielectric layer and the hydrophobic layer of the EWOD device fabricated through the printing process and the solution-based process. First of all, the sheet resistance, surface shape and surface roughness of the printed electrode were measured. The sheet resistance of the printed electrode after its heat treatment was measured with a four-point probe and was approximately 0.7 Ω . The thickness of the electrode was measured with Alpha-step equipment using 20 identical samples. Measurement revealed that the thickness was about 470 nm. A scanning electron microscopy (SEM) was used to observe the shape of the electrode. The cross-section and surface of the electrode were examined (Fig. 5). The thickness of the printed electrode surface was uniform as a whole. However, there were some unfilled spots on the surface (Fig. 5(c)). Magnifying the surface of the electrode (Fig. 5(d)) revealed that irregular wrinkle-like patterning. Equipment from AFM was used to measure the surface roughness of the electrode, and the size of the specimen measured was 5 μ m \times 5 μ m. The Root Mean Square (RMS) roughness of the electrode surface was measured to be about 6.5 nm (red line in Fig. 6) and 7.8 nm (green line in Fig. 6). In general, the surface roughness increases a contact angle hysteresis, requiring a higher operation voltage to transport droplets on the EWOD electrode.²¹⁻²³ So we try to make the surface roughness value minimum in the fabrication process.

The thickness, shape and performance of the dielectric layer were measured. The thickness, when measured using apparatuses from Alpha-step and SEM (Fig. 5(a)), was 1.6 μ m. The cross-section of the

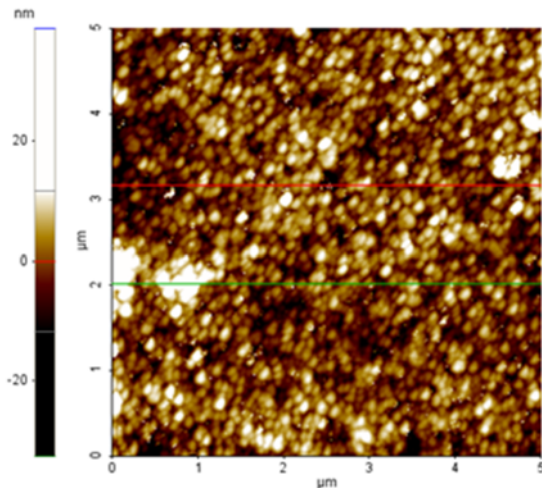


Fig. 6 AFM image of a printed electrode surface (Scan area is $5\ \mu\text{m} \times 5\ \mu\text{m}$. Along the red and green lines, the RMS roughness is measured)

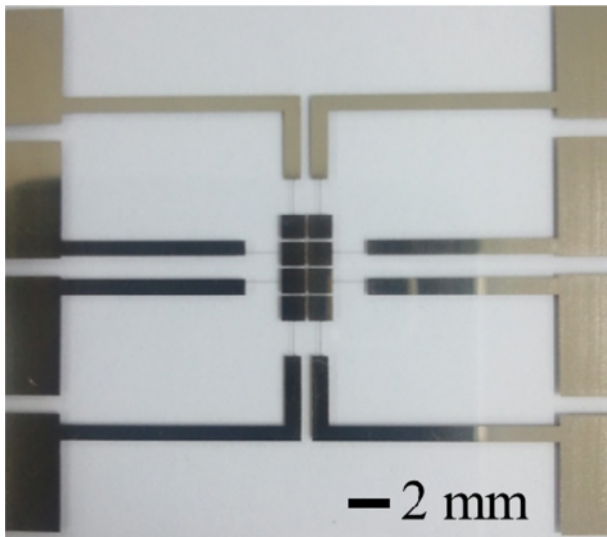


Fig. 7 Fabrication result of an electrode for the printed EWOD device

EWOD device (Fig. 5(a)) was examined by means of equipment from SEM to grasp how the dielectric layer was coated over the electrode. The layer was found coated thinly and uniformly. The dielectric strength of the layer was measured using a Keithley 4200 semiconductor parameter analyzer. To measure the properties of the dielectric layer, a specimen was prepared as follows: Gold (Au) was deposited over a silicon wafer, over which a dielectric layer was spin-coated. Gold (Au) was deposited again over the spin-coated surface to make a metal-insulator-metal configuration. Measurement revealed that the dielectric strength was about 100 V/mm.

Since the Teflon solution was coated on the surfaces of both the base plate and the top cover plate, the thickness of the hydrophobic layer was measured using equipment from Alpha-step after it was spin-coated on the glass substrate and the ITO-coated glass. When the Teflon solution was spin-coated over the glass substrate and the ITO-coated glass at 2000 rpm, the thickness of the hydrophobic layer for

both surfaces was less than 100 nm at 60 nm and 90 nm, respectively.

3.5 Printed EWOD device

Fig. 7 shows an electrode fabricated on a $50\ \text{mm} \times 50\ \text{mm}$ glass substrate via the ROP method. The size of this electrode to be used as the base plate of a two-parallel plate EWOD device is finally as follows: the size of one electrode at the 2×4 electrode array was $1.41\ \text{mm} \times 1.41\ \text{mm}$; the gap between two discrete electrodes was 170 μm (which can be reduced to 50 μm); and the width of the line electrode connecting between the electrode array and the pad electrode was 10 μm (which can be increased to 100 μm for easy fabrication). When we make the size of the pad electrode and side electrode smaller, we can fabricate many (~ 15) EWOD devices with a square glass substrate of $50\ \text{mm} \times 50\ \text{mm}$ used in this experiment. The cover plate was fabricated by spin-coating Teflon solution over the ITO-coated glass substrate.

4. Droplet Transport on Printed EWOD Device

4.1 Experimental setup

A droplet transport experiment was conducted using a two-parallel plate EWOD device. The electrode specimen used as a base plate was a 2×4 electrode array as shown in Fig. 6 while the electrode used as a cover plate was an ITO-coated glass specimen. The thickness of the ITO electrode is 200 nm. A 3M double coated tape with a thickness of 500 μm was used a spacer between the base and the cover plates. The liquid of a droplet was distilled water and its size was 2 μL . A function generator (33220 A, Agilent) and an amplifier were used to apply voltage to the droplet. The magnitude of the AC voltage applied was 40-100 Vrms and the frequency was 1 Hz~1 kHz. The droplet transport experiment was conducted in ambient air, and a new droplet was used for each experiment.

4.2 Results and discussion

The threshold voltage for droplet transport in the EWOD device was determined experimentally. A droplet was placed on the base plate and the cover plate was placed over it. Then ground (GND) and high voltages were applied to the two electrodes patterned on the base plate while the top ITO plate is in a floating state. The movement of the droplet was observed. The droplet started to move when the voltage applied was 70 Vrms. However, when GND voltage was applied to the top ITO cover plate and high voltage was applied to the electrode of the base plate, the threshold voltage for droplet transport was reduced to 40 Vrms.

Fig. 8 shows that the droplets were transported freely to the electrode array. Droplets were successfully transported moving clockwise on four electrodes with 2×2 arrays when the voltage applied were 40 Vrms and 10 Hz (Fig. 8(a)). Droplets were also successfully transported linearly on 2×4 arrays when the voltage applied were 70 V DC (Fig. 8(b)). All these droplet transport results suggest that EWOD devices can be fabricated through a printing process and a solution-based process.

Next we investigate the effect of the frequency of the applied AC voltage on droplet transport. The droplet was transported on the electrode when AC voltage of 70 Vrms was applied at a low frequency (< 100 Hz). However, it was not transported at a high frequency of 1 kHz or

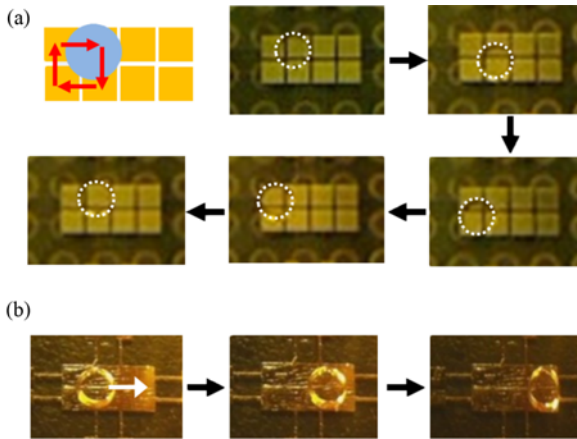


Fig. 8 Transport of a droplet on printed EWOD device: (a) Round movement of a droplet at 40 Vrms and 10 Hz and (b) straight movement of a droplet at 70 V DC

higher. The reason is presumed to be that the gap between the two discrete electrodes is too large for the droplet to go over. We consider that this problem can be solved when each discrete electrode has branches overlapping with adjacent electrodes for the droplet to contact with the surface of the next electrode.²⁴

To determine the performance of our EWOD device, we compare our result with the Pollack's work¹⁶ with respect to electrowetting number ($\eta = \epsilon_0 \epsilon_d V^2 / (2d\gamma)$). (See the middle part of Eq. (1)) The electrowetting number measures the strength of the electrostatic energy compared to surface tension.² From the threshold voltage value, the electrowetting number indicates the required threshold electrical energy for droplet transport on the EWOD device given. In the work of Pollack et al.,¹⁶ the threshold voltage for droplet transport with the parallel-plate EWOD configuration is about 40 V, which corresponds to the electrowetting number of ~ 0.44 . In our system, the threshold voltage is about 40 V, which corresponds to the electrowetting number of ~ 0.24 . These results show that the performance of droplet control in our printed EWOD device system is compatible with previous works.

This study explored the possibility of using a printing process and a solution-based process to fabricate the EWOD device and has demonstrated that droplets are actually transported on the device. Compared to those fabricated through the traditional semiconductor process,¹⁶ the EWOD device fabricated through a printing process and a solution-based process show no notable difference in the droplet transport performance. Printing quality of each layer of the EWOD device is good in terms of surface roughness, thickness, uniformity. In addition, the ability of the printing process to allow for large area tasks and save costs will make it possible for it to be used in the fabrication of affordable large area lab-on-a-chips.

5. Conclusion

This paper shows how EWOD devices can be fabricated through a printing process and a solution-based process. Reverse offset printing (ROP) process that can regulate the thickness and surface roughness of the printout was used to fabricate an electrode of the EWOD device.

The thickness of the electrode was around 470 nm and the surface roughness (Ra) was around 5.3 nm. The dielectric layer and the hydrophobic layer were fabricated via a solution-based process. The dielectric material of PVP solution is more affordable and has greater dielectric constant (3.9) and higher dielectric strength (~ 100 V/mm) than the dielectric materials (Teflon, PDMS, Polyimide) that are commonly used for solution-based process. Spin coating was used to regulate the thickness of the dielectric layer. Droplets were successfully moving at the small magnitude of voltage of 40 to 70 Vrms with a frequency of 10 Hz in the 8 cell (2×4) EWOD device.

Additional studies are planned which focus on making the best of the printing process to fabricate EWOD devices on large area flexible plates. Such studies will also be directed towards showing that basic droplet manipulation required for a lap-on-a-chip, including not only droplet transport but also dispensing, splitting and merging, is feasible. The fabrication of a single plate type, in addition to a two-plate type, is also planned as a research paper in the short-term.

ACKNOWLEDGEMENT

We would like to acknowledge the financial support from the R&D Convergence Program of MSIP (Ministry of Science, ICT and Future Planning) and ISTK (Korea Research Council for Industrial Science and Technology) of Republic of Korea (Grant B551179-12-02-00).

REFERENCES

1. Kang, K. H., "How Electrostatic Fields Change Contact Angle in Electrowetting," *Langmuir*, Vol. 18, No. 26, pp. 10318-10322, 2002.
2. Mugele, F. and Baret, J. C., "Electrowetting: From Basics to Applications," *Journal of Physics: Condensed Matter*, Vol. 17, No. 28, p. R705, 2005.
3. Kuiper, S. and Hendriks, B., "Variable-Focus Liquid Lens for Miniature Cameras," *Applied Physics Letters*, Vol. 85, No. 7, pp. 1128-1130, 2004.
4. Smith, N. R., Abeyasinghe, D. C., Haus, J. W., and Heikenfeld, J., "Agile Wide-Angle Beam Steering with Electrowetting Microprisms," *Optics Express*, Vol. 14, No. 14, pp. 6557-6563, 2006.
5. Hayes, R. A. and Feenstra, B. J., "Video-Speed Electronic Paper based on Electrowetting," *Nature*, Vol. 425, No. 6956, pp. 383-385, 2003.
6. Cho, S. K., Moon, H., and Kim, C. J., "Creating, Transporting, Cutting, and Merging Liquid Droplets by Electrowetting-based Actuation for Digital Microfluidic Circuits," *Microelectromechanical Systems, Journal of*, Vol. 12, No. 1, pp. 70-80, 2003.
7. Boeuf, J., "Plasma Display Panels: Physics, Recent Developments and Key Issues," *Journal of Physics D: Applied Physics*, Vol. 36, No. 6, p. R53, 2003.
8. Menard, E., Meitl, M. A., Sun, Y., Park, J. U., Shir, D. J. L., et al.,

- “Micro-and Nanopatterning Techniques for Organic Electronic and Optoelectronic Systems,” *Chemical Reviews*, Vol. 107, No. 4, pp. 1117-1160, 2007.
9. Krebs, F. C., Gevorgyan, S. A., and Alstrup, J., “A Roll-to-Roll Process to Flexible Polymer Solar Cells: Model Studies, Manufacture and Operational Stability Studies,” *Journal of Materials Chemistry*, Vol. 19, No. 30, pp. 5442-5451, 2009.
 10. Yu, J. S., Kim, I., Kim, J. S., Jo, J., Larsen-Olsen, T. T., et al., “Silver Front Electrode Grids for Ito-Free all Printed Polymer Solar Cells with Embedded and Raised Topographies, Prepared by Thermal Imprint, Flexographic and Inkjet Roll-to-Roll Processes,” *Nanoscale*, Vol. 4, No. 19, pp. 6032-6040, 2012.
 11. Yang, L., Rida, A., Vyas, R., and Tentzeris, M. M., “RFID Tag and RF Structures on a Paper Substrate using Inkjet-Printing Technology,” *IEEE Transactions on Microwave Theory and Techniques*, Vol. 55, No. 12, pp. 2894-2901, 2007.
 12. Zhao, X., Chu, B. T., Ballesteros, B., Wang, W., Johnston, C., et al., “Spray Deposition of Steam Treated and Functionalized Single-Walled and Multi-Walled Carbon Nanotube Films for Supercapacitors,” *Nanotechnology*, Vol. 20, No. 6, Paper No. 065605, 2009.
 13. Kim, M., Koo, J. B., Baeg, K. J., Jung, S. W., Ju, B. K., and You, I. K., “Top-Gate Staggered Poly (3,3-Dialkyl-Quarterthiophene) Organic Thin-Film Transistors with Reverse-Offset-Printed Silver Source/ Drain Electrodes,” *Applied Physics Letters*, Vol. 101, No. 13, Paper No. 133306, 2012.
 14. Liu, H., Dharmatilleke, S., Maurya, D. K., and Tay, A. A., “Dielectric Materials for Electrowetting-on-Dielectric Actuation,” *Microsystem Technologies*, Vol. 16, No. 3, pp. 449-460, 2010.
 15. Yi, U. C. and Kim, C. J., “Characterization of Electrowetting Actuation on Addressable Single-Side Coplanar Electrodes,” *Journal of Micromechanics and Microengineering*, Vol. 16, No. 10, pp. 2053-2059, 2006.
 16. Pollack, M. G., Fair, R. B., and Shenderov, A. D., “Electrowetting-based Actuation of Liquid Droplets for Microfluidic Applications,” *Applied Physics Letters*, Vol. 77, No. 11, pp. 1725-1726, 2000.
 17. Jang, Y., Lee, W. H., Park, Y. D., Kwak, D., Cho, J. H., and Cho, K., “High Field-Effect Mobility Pentacene Thin-Film Transistors with Nanoparticle Polymer Composite/Polymer Bilayer Insulators,” *Applied Physics Letters*, Vol. 94, No. 18, Paper No. 183301, 2009.
 18. Klauk, H., Halik, M., Zschieschang, U., Schmid, G., Radlik, W., and Weber, W., “High-Mobility Polymer Gate Dielectric Pentacene Thin Film Transistors,” *Journal of Applied Physics*, Vol. 92, No. 9, pp. 5259-5263, 2002.
 19. Abdelgawad, M. and Wheeler, A. R., “Rapid Prototyping in Copper Substrates for Digital Microfluidics,” *Advanced Materials*, Vol. 19, No. 1, pp. 133-137, 2007.
 20. Kim, I., Kwak, S. W., Kim, K. S., Lee, T. M., Jo, J., et al., “Effect of Ink Cohesive Force on Gravure Offset Printing,” *Microelectronic Engineering*, Vol. 98, pp. 587-589, 2012.
 21. Gupta, R., Sheth, D. M., Boone, T. K., Sevilla, A. B., and Fréchet, J., “Impact of Pinning of the Triple Contact Line on Electrowetting Performance,” *Langmuir*, Vol. 27, No. 24, pp. 14923-14929, 2011.
 22. Li, F. and Mugele, F., “How to Make Sticky Surfaces Slippery: Contact Angle Hysteresis in Electrowetting with Alternating Voltage,” *Applied Physics Letters*, Vol. 92, No. 24, pp. 244108, 2008.
 23. Nelson, W. C., Sen, P., and Kim, C. J. C., “Dynamic Contact Angles and Hysteresis under Electrowetting-on-Dielectric,” *Langmuir*, Vol. 27, No. 16, pp. 10319-10326, 2011.
 24. Park, J. K., Lee, S. J., and Kang, K. H., “Fast and Reliable Droplet Transport on Single-Plate Electrowetting on Dielectrics using Nonfloating Switching Method,” *Biomicrofluidics*, Vol. 4, No. 2, Paper No. 024102, 2010.